Frequency-Dependent Characteristics of an Ion-Implanted GaAs MESFET with Opaque Gate Under Illumination

Nandita Saha Roy, B. B. Pal, and R. U. Khan

***Abstract*—Commercial metal–semiconductor–field-effect transistors (MESFET's) have opaque gate. We present here the frequency-dependent characteristics of an ion-implanted GaAs MESFET with opaque gate under illumination. The incident light enters the device through the gate-source and gate-drain spacings. Two photovoltages are developed: one across the Schottky junction due to generation in the side walls of the depletion layer below the gate and the other across the channel-substrate junction due to generation in the channel-substrate depletion region. The frequency dependence of the two photovoltages along with channel charge, drain-source current, transconductance and channel conductance of the device have been studied analytically and compared with the published theoretical results. For the first time, a commercially available GaAs optically illuminated field-effect transistor (OPFET) has been analyzed for frequency-dependent characteristics instead of the transparent/semitransparent gate OPFET.**

***Index Terms*—AC model optically illuminated field-effect transistor (OPFET), GaAs OPFET, optically controlled metal–semiconductor–field-effect transistor (MESFET).**

I. Introduction

GALLIUM arsenide (GaAs) metal–semiconductor–field-effect transistors (MESFET's), over the recent years, have been extensively studied and developed for its high-speed and low-power applications. MESFET being an optically sensitive microwave element can be treated as a dual gate device under optically illuminated field-effect transistor (OPFET) in which the real gate is electrical and the virtual gate is optical. The potentiality of such GaAs MESFET as a high speed optical transducer was first shown by Baack *et al.* [1]. Application of GaAs MESFET as an optically switched amplifier and also as optical/microwave transformer was experimentally found by Mizuno [2]. Analysis of GaAs OPFET has been carried out over the years under both dc and ac conditions. Mishra *et al.* [3] first presented theoretically the frequency-dependent characteristics of an ion-implanted GaAs OPFET. The analysis, however, neglects the photovoltaic effect at the Schottky junction and the active-layer substrate junction. The signal modulated ion-implanted GaAs OPFET characteristics considering the photovoltage developed across the Schottky junction and the gate width modulation have been reported by Pal *et al.* [4]. In that work, the gate has been considered transparent or semitransparent to radiation which is not true for commercially available MESFET's. Commercial MESFET's have gate opaque to optical radiation.

Recently a dc analysis has been published for an ion-implanted GaAs MESFET under illuminated condition with opaque gate. The light enters the device through the spacings of source, gate and drain. Hence, the absorption of photons takes place in the side walls of the gate depletion region (arc region), channel neutral region, channel-substrate depletion region and substrate neutral region. As a result, an external photovoltage is developed across the Schottky junction and an internal photovoltage is developed across the channel-substrate junction. These two photovoltages lead to channel conductivity modulation of the device. In the present paper, we propose to study analytically the effect of frequency modulated optical signal on the GaAs MESFET with opaque gate. The ion-implanted profile in the channel have been considered to be represented by the Gaussian profile [6]. When the modulated optical signal is incident on the device, the carriers generated at different regions are also modulated at the same frequency. There is no generation of electron-hole pairs just below the gate. The excess electrons due to photogeneration move toward the channel to contribute to the drain-source current along with that contributed by the impurity electrons. The photogenerated holes develop the photovoltage across the two junctions. The variation of the drain current, the photovoltages and the transconductance with frequency have been studied and compared with published theoretical results. The theory is given below.

II. Theory

The schematic structure of the device is shown in Fig. 1(a). The drain-source current flows along the x-direction and the device is illuminated along the y-direction. The gate being opaque, the excess carriers are generated in the extended gate depletion region (side walls), the neutral region of the channel and the depletion region at the active layer-substrate junction (the substrate thickness is such that it gets totally depleted).

The optically generated electrons flow toward the channel by diffusion and recombination in the neutral region and by drift and recombination in the depletion region and contribute to the drain-source current when a drain source voltage is applied. The holes on the other hand move in the opposite direction, developing a forward voltage across the junctions: an external photovoltage across the Schottky junction due to generation in the sidewalls of the gate depletion regions and an in-

Manuscript received April 15, 1999; revised September 10, 1999.

The authors are with the Department of Electronics Engineering, Institute of Technology, Banaras Hindu University, Varanasi 221005, India.

Publisher Item Identifier S 0733-8724(00)01365-7.

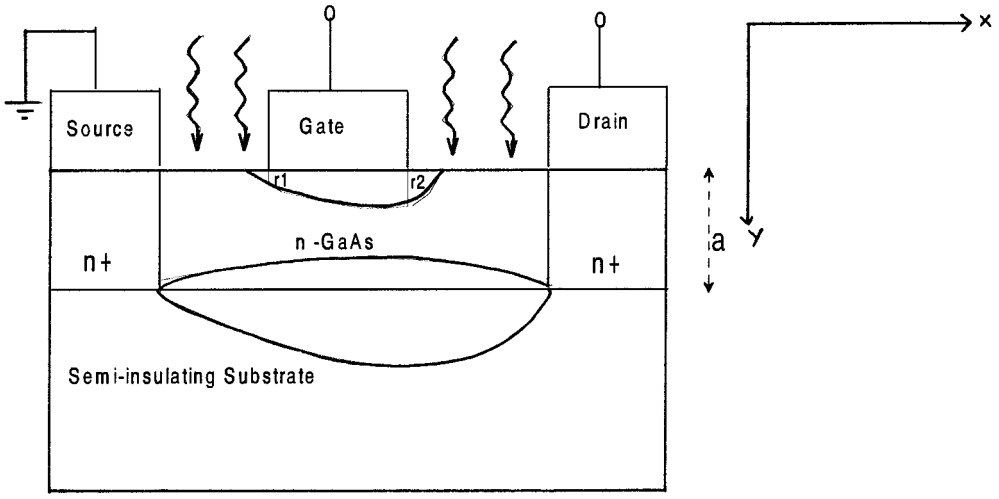

(a)

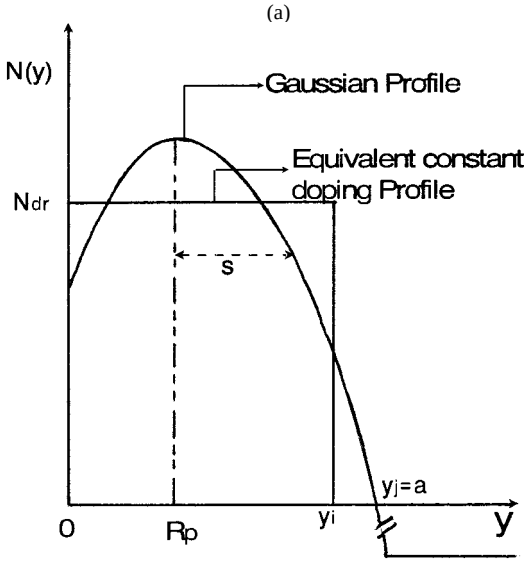

(b)

Fig. 1. (a) Schematic structure of the device and (b) Gaussian profile and its equivalent constant doping distribution of impurities in the active layer.

ternal photovoltage across the channel-substrate depletion region due to generation of holes in the corresponding depletion region. Two photovoltages greatly modulate the channel thickness enhancing the flow of carriers significantly due to impurity electrons in addition to photogenerated electrons.

The ion-implanted profile in the active region of the device is represented by the Gaussian distribution, given by [6]

$$N(y) = \frac{Q}{\sigma\sqrt{2\pi}} \exp\left[-\left(\frac{y - R_p}{\sigma\sqrt{2}}\right)^2\right] \tag{1}$$

where

Q implanted dose;
σ straggle parameter;
R_P projected range.

The number of photogenerated electrons and holes are obtained by solving the continuity equations [9],

$$\frac{\partial n(y,\,t)}{\partial t} = \frac{1}{q}\frac{\partial J_n(y,\,t)}{\partial y} + G - \frac{n(y,\,t)}{\tau_n} - \frac{R_s\tau_n}{S_n} \tag{2}$$

for electrons

$$\frac{\partial p(y,\,t)}{\partial t} = -\frac{1}{q}\frac{\partial J_p(y,\,t)}{\partial y} + G - \frac{p(y,\,t)}{\tau_p} - \frac{R_s\tau_p}{S_p} \tag{3}$$

for holes, where

τ_n lifetime for electrons;
τ_p lifetime for holes;
J_n electron current densities;
J_p hole current densities;

and are represented by

$$J_n = qv_y n + qD_n\frac{\partial n}{\partial y} \tag{4}$$

$$J_p = qv_y p - qD_p\frac{\partial p}{\partial y} \tag{5}$$

G volume generation rate;
D_n and D_p diffusion coefficients for electrons and holes;
n and p excess electron and hole concentrations;

v_y carrier velocity along the vertical y-direction perpendicular to the surface of the device and is assumed same as the scattering limited velocity [3];
S_n and S_p surface recombination velocities for electrons and holes;
R_s surface recombination rate.

The term R_s is calculated using the expression [3]

$$R_s = \frac{N_T k_n k_p (n_s p_s - n_t p_t)}{k_n (n_s + n_t) + k_p (p_s + p_t)} \tag{6}$$

where
n_s $\alpha\phi\tau_n$;
p_s $\alpha\phi\tau_p$;
and other terms have the same meaning as in [3].

The optical flux density being assumed to be modulated by the signal frequency, under small signal condition we write

$$\phi = \phi_o + \phi_1 e^{j\omega t} \tag{7.a}$$
$$n = n_o + n_1 e^{j\omega t} \tag{7.b}$$
$$p = p_o + p_1 e^{j\omega t} \tag{7.c}$$
$$G = G_o + G_1 e^{j\omega t} \tag{7.d}$$

where "zero" indicates the dc value and "one" indicates the ac value.

Assuming that only negative trap centers are present and that the traps close to the surface are important, (6) may be approximated as

$$R_s \approx N_t k_p p_s$$

or

$$R_s = (N_T k_p \alpha \phi_o \tau_p) + (N_T k_p \alpha \tau_p \phi_1 e^{j\omega t}). \tag{8}$$

Substitution of (4), (5), (7), and (8) into (2) and (3) provides two sets of differential equations under dc and ac conditions.

A. Calculation of the Photovoltage

Due to illumination, the photovoltage is developed across i) the Schottky junction (V_{op1}) called the external photovoltage and ii) the active layer-substrate junction (V_{op2}) called the internal photovoltage.

The transport mechanism in the depletion region being drift and recombination, the continuity equation for the carriers is given by a first order differential equation. For holes it is written as

$$\frac{\partial p}{\partial t} = -\frac{\partial p}{\partial y} - \frac{p}{v_y \tau_p} + \frac{\alpha\phi}{v_y} e^{-\alpha y} - \frac{R_s \tau_p}{S_p v_y}. \tag{9}$$

Equation (9) is solved under ac condition resulting a solution for hole density as

$$p(y) = \frac{\alpha\phi_1\tau_{\omega p}}{(1 - \alpha v_y \tau_{\omega p})} e^{-\alpha y} - \frac{N_T k_p \tau_p \tau_{\omega p} \phi_1 \alpha}{S_p} + C \exp\left(-\frac{y}{v_y \tau_{\omega p}}\right) \tag{10}$$

where
$1/\tau_{\omega p}$ $1/\tau_p + j\omega$;
$\tau_{\omega p}$ lifetime of holes under ac condition;
$\tau_{\omega p}$ is independent of ω if $1/\tau_p \gg \omega$.

The constant C of (10) is evaluated using the boundary condition at

$$y = y_{dg}, \qquad p = \alpha\phi_1\tau_{\omega p} e^{-\alpha y_{dg}}$$

where y_{dg} is the extension of the gate depletion region in the channel measured from the surface.

The sidewalls of the gate depletion region are assumed quarter arcs.

Considering the arcs at the source and drain ends to have radii r_1 and r_2, respectively, where

$$r_1 = [y_{dg}]_{v(x)=0}, \qquad r_2 = [y_{dg}]_{v(x)=v_{ds}}$$

the number of holes crossing the junction at $y = 0$ is given by [5]

$$p(0) = \frac{\pi}{4} Z (p_1 r_1^2 + p_2 r_2^2) \tag{11}$$

where

$$p_1 = \alpha\phi_1\tau_{\omega p} e^{-\alpha r_1} \quad \text{and} \quad p_2 = \alpha\phi_1\tau_{\omega p} e^{-\alpha r_2}.$$

The external photovoltage across the Schottky junction is obtained using the relation

$$V_{op1} = \frac{kT}{q} \ln\left(\frac{J_p}{J_s}\right) = \frac{kT}{q} \ln\left(\frac{q v_y p(0)}{J_{s1}}\right) \tag{12}$$

where J_{s1} is the reverse saturation current density across the Schottky junction.

Similarly, the photovoltage developed across the active layer-substrate junction is calculated from the relation

$$V_{op2} = \frac{kT}{q} \ln\left(\frac{J_p}{J_s}\right) = \frac{kT}{q} \ln\left(\frac{q v_y p(a)}{J_{s2}}\right) \tag{13}$$

where
$p(a)$ number of holes crossing the junction at $y = a$;
J_{s2} reverse saturation current density for the channel-substrate junction.

$p(a)$ is calculated considering only the region from which the generated holes cross the junction at $y = a$. In the present structure it is the depletion region of the channel-substrate junction extended in the channel. The corresponding differential equation is given by

$$\frac{\partial p}{\partial t} = -\frac{\partial p}{\partial y} - \frac{p}{v_y \tau_p} + \frac{\alpha\phi}{v_y} e^{-\alpha y} \tag{14}$$

where the recombination due to traps in the substrate region is neglected.

Equation (14) has the solution given by

$$p(y) = \frac{\alpha\phi_1\tau_{\omega p}}{(1 - \alpha v_y \tau_{\omega p})} e^{-\alpha y} + C' \exp\left(-\frac{y}{v_y \tau_{\omega p}}\right) \tag{15}$$

where C' is a constant and is evaluated using the condition at

$$y = y_{ds}, \qquad p(y_{ds}) = \alpha\phi_1\tau_p e^{-\alpha y_{ds}}$$

y_{ds} is the extension of the n–p junction depletion region in the channel measured from the surface. The calculation of the photovoltages is important because they modify the depletion width y_{dg} and y_{ds}. Using the abrupt junction approximation y_{dg} and y_{ds} under dark and illumination are calculated as given below [6]

$$y_{dg} = \left[\frac{2\varepsilon}{qN_{dr}}\left(\phi_B - \Delta + v(x) - v_{gs}\right)\right]^{1/2} \tag{16}$$

where N_{dr} is the constant doping concentration in the active region equivalent to the ion-implanted profile. N_{dr} is calculated using the relation [Fig. 1(b)]

$$N_{dr}y_i = \int_0^{y_j} \frac{Q}{\sigma\sqrt{2\pi}} \exp\left[-\left(\frac{y-R_p}{\sigma\sqrt{2}}\right)^2\right] dy \tag{17}$$

where

- y_i distance for which $N_{dr}y_i$ is same as that of implanted charge in the channel;
- y_j junction depth of the active region from the surface which is same as "a," the active layer thickness.

Under illumination y_{dg} is modified to y'_{dg} given by

$$y'_{dg} = \left[\frac{2\varepsilon}{qN_{dr}}(\phi_B - \Delta + v(x) - v_{gs} - v_{op1})\right]^{1/2} \tag{18}$$

y_{ds} is expressed as

$$y_{ds} = a - \frac{N_A}{N_{dr}}\left[\frac{2\varepsilon}{qN_A}\left(v_{bi} + v(x) - v_{bs}\right)\right]^{1/2} \tag{19}$$

under dark and becomes

$$y'_{ds} = a - \frac{N_A}{N_{dr}}\left[\frac{2\varepsilon}{qN_A}\left(v_{bi} + v(x) - v_{bs} - v_{op2}\right)\right]^{1/2} \tag{20}$$

under illumination. Thus, the drain-source current changes as the photovoltage gets modified by the signal frequency. In (16)–(20), $v(x)$ is the channel voltage, ϕ_B is the Schottky barrier height, Δ is the position of fermi level at the neutral region below the conduction band, v_{bi} is the built in voltage across the n–p junction, v_{bs} is the substrate potential and N_A is the substrate concentration.

B. Calculation of Channel Charge

The total channel charge is due to the carriers present because of ion-implantation and optical generation, i.e

$$Q_{\text{total}} = Q_{\text{ion}} + Q_{\text{illumination}}. \tag{21}$$

The charge is calculated using the relation

$$Q(y) = q\int N(y)\,dy.$$

1) Charge Due to Ion-Implantation: The channel charge due to ion-implantation is given by

$$Q_{\text{ion}} = q\int_{y'_{dg}}^{y'_{ds}} N(y)\,dy. \tag{22}$$

$N(y)$ being given by (1). Substituting $N(y)$ in (22), we obtain

$$Q_{\text{ion}} = q\left[-\frac{Q}{2}\operatorname{erf}\left\{\frac{(y'_{dg}-R_p)}{\sigma\sqrt{2}}\right\} + \frac{Q}{2}\operatorname{erf}\left\{\frac{(y'_{ds}-R_p)}{\sigma\sqrt{2}}\right\}\right]. \tag{23}$$

2) Charge Due to Carriers Generated in the Neutral Channel Region: When the frequency modulated optical signal is incident on the device, the number of generated electrons are obtained by solving (3). Since the transport mechanism is diffusion and recombination for the neutral region in absence of any drain-source voltage the continuity equation is a second order differential equation.

The ac equation is given by

$$\frac{d^2n_1}{dy^2} - \frac{n_1}{D_n\tau_{\omega n}} = -\frac{\alpha\phi_1 e^{-\alpha y}}{D_n} \tag{24}$$

in which $1/\tau_{\omega n} = 1/\tau_n + j\omega$. $\tau_{\omega n}$ is the lifetime of electrons under ac condition. $\tau_{\omega n}$ is independent of ω if $1/\tau_n \gg \omega$.

Since only the presence of negative traps have been assumed at or close to the surface the surface recombination term is absent in the continuity equation for electrons.

The solution to the above equation is,

$$n_1 = \alpha\phi_1\left[\tau_{\omega n} + \frac{1}{D_n\left(\alpha^2 - \frac{1}{L_{n\omega}^2}\right)}\right]\exp\left(-\frac{y}{L_{n\omega}}\right) - \frac{\alpha\phi_1 e^{-\alpha y}}{D_n\left(\alpha^2 - \frac{1}{L_{n\omega}^2}\right)} \tag{25}$$

where the boundary condition applied is at $y = 0$, $n = \alpha\phi\tau_{\omega n}$, $L_{n\omega} = \sqrt{D_n\tau_{\omega n}}$ and is called the ac diffusion length of electrons.

The charge developed due to the electrons generated in this region is given by,

$$Q_{\text{neutral}} = q\int_{y_{dg}}^{y_{ds}} n_1\,dy.$$

Substituting n_1 and integrating we get

$$Q_{\text{neutral}} = q\alpha\phi_1 L_{n\omega}\left[\tau_{\omega n} + \frac{1}{D_n\left(\alpha^2 - \frac{1}{L_{n\omega}^2}\right)}\right] \cdot \left[\exp\left(-\frac{y_{dg}}{L_{n\omega}}\right) - \exp\left(-\frac{y_{ds}}{L_{n\omega}}\right)\right] + \frac{\phi_1}{D_n\left(\alpha^2 - \frac{1}{L_{n\omega}^2}\right)}\left[\exp(-\alpha y_{ds}) - \exp(-\alpha y_{dg})\right]. \tag{26}$$

3) Charge Due to Carriers Generated in the Depletion Region: The number of carriers generated in the depletion region is obtained by solving the continuity equation for electrons which is similar to (10), except that the surface recombination term is absent.

The solution is given by

$$n_{1dep} = \frac{\alpha\phi_1\tau_{\omega n}}{(1+\alpha v_y\tau_{\omega n})}\, e^{-\alpha y}. \tag{27}$$

The charge developed due to electrons contributed from the side walls of the gate depletion region (arc regions) is given by,

$$Q_{dep1} = qZ\,\frac{\pi}{4}\left[\int_0^{r_1} n_{1dep}\,dy + \int_0^{r_2} n_{1dep}\,dy\right] \tag{28}$$

and is evaluated as

$$Q_{dep1} = qZ\frac{\pi}{4}\left[\frac{\phi_1\tau_{\omega n}}{(1+\alpha v_y\tau_{\omega n})}\left[1-\exp(-\alpha r_1)\right] + \frac{\phi_1\tau_{\omega n}}{(1+\alpha v_y\tau_{\omega n})}\left[1-\exp(-\alpha r_2)\right]\right]. \tag{29}$$

The charge in the n–p$^-$ junction depletion region due to generation of electrons is given by

$$Q_{dep2} = q\int_{y_{ds}}^{y_w} n_{2dep}\,dy \tag{30}$$

where y_w is the extension of the channel-substrate depletion region in the substrate measured from the surface. n_{2dep} is same as in (27). Substituting (27) in (30) one obtains

$$Q_{dep2} = \frac{q\phi_1\tau_\omega}{(1+\alpha v_y\tau_\omega)}\left\{e^{-\alpha y_{ds}} - e^{-\alpha y_w}\right\} \tag{31}$$

y_w is given by

$$y_w = y_{ds} + \left[\frac{2\varepsilon}{qN}\left(v_{bi}+v_{ds}-v_{bs}\right)\right]^{1/2}$$

in which

$$\frac{1}{N} = \frac{1}{N_A} + \frac{1}{N_{dr}}.$$

C. Calculation of Drain-Source Current

The drain-source current is calculated from gradual channel approximation using the relation,

$$I_{ds} = \frac{\mu Z}{L}\int_0^{v_{ds}} Q_{\text{total}}\,dv \tag{32}$$

where Q_{total} is given by (21).

Thus, substituting (23), (26), (29), and (31) in (32) and integrating we obtain the total drain-source current of the opaque gate OPFET.

The contribution to the drain-source current (I_{ds}) due to ion-implantation is given by

$$I_{\text{ion}} = \frac{q\mu Z}{L}\left[-\frac{Q}{2}\,I_1 + \frac{Q}{2}\,I_2\right] \tag{33}$$

where I_1 and I_2 are given in the Appendix.

In the neutral channel region, the ac drain-source current is obtained as

$$I_{\text{neutral}} = \frac{q\mu Z}{L}\left[\alpha\phi_1 L_{n\omega}\left\{\tau_{\omega n}+\frac{1}{A}\right\}(I_3-I_4) + \frac{\phi_1}{A}\,(I_5-I_6)\right] \tag{34}$$

I_3, I_4, I_5, and I_6 being given in the Appendix and $A = D_n(\alpha^2 - (1/L_{n\omega}^2))$.

The current contribution due to generation in the sidewalls of the gate depletion layer is given by,

$$I_{dsdep1} = I_{ds1} + I_{ds2}$$

where

$$I_{ds1} = qv_dZ\,\frac{\pi}{4}\int_0^{r_1} n_{1dep}\,dy$$

and

$$I_{ds2} = qv_sZ\,\frac{\pi}{4}\int_0^{r_2} n_{1dep}\,dy \tag{35}$$

v_d drift velocity of carriers at the source end and equals to μE;
μ low field mobility ;
E applied field ($E = -(dv/dx)$);
v_s saturated velocity at the drain end.

Substituting (27) in (35), we obtain

$$I_{ds1} = -\frac{q\mu Z\pi}{4L}\left\{\frac{\phi_1\tau_{\omega n}}{(1+\alpha v_y\tau_{\omega n})}\left[1-\exp(-\alpha r_1)\right]\right\}V_{ds} \tag{36}$$

and

$$I_{ds2} = \frac{qv_sZ\pi}{4}\left\{\frac{\phi_1\tau_{\omega n}}{(1+\alpha v_y\tau_{\omega n})}\left[1-\exp(-\alpha r_2)\right]\right\}. \tag{37}$$

I_{ds1} drain current contributed by the arc regions at the source end;
I_{ds2} drain current due to the arc region at the drain end of the gate depletion region.

The drain-source current due to generation at the n–p junction depletion region is calculated substituting (31) in (32).

Thus

$$I_{dsdep2} = \frac{q\mu Z}{L}\left[\frac{q\phi_1\tau_{\omega n}}{\alpha\varepsilon(1+\alpha v_y\tau_{\omega n})}\left\{I_7 - I_8\right\}\right] \tag{38}$$

where I_7 and I_8 are given in the Appendix.

So the total drain-source current (I_{ds}) is obtained by summing up the (33), (34), (36)–(38)

$$I_{ds} = I_{\text{ion}} + I_{\text{channel}} + I_{dsdep1} + I_{dsdep2}. \tag{39}$$

The dependence of frequency of I_{ds} through different components arises due to the ac lifetime and ac diffusion length of electrons and holes. The frequency limitation depends on the conditions that $1/\tau_n,\ 1/\tau_p \gg \omega$. When ω is larger than or comparable with $1/\tau_n$ or $1/\tau_p$, the frequency effect dominates. Further, (39) represents the current for an opaque gate OPFET. For transparent or semitransparent gate OPFET, the component I_{dsdep1} will be modified. In that case, it will also include the generation of carriers just below the gate depletion region in addition to that of the extended arc regions. This has already been discussed in [10] under dc condition.

D. Calculation of Transconductance and Channel Conductance

The transconductance and channel conductance of the device are calculated using the following relations,

$$g_m = \left[\frac{dI_{ds}}{dV_{gs}}\right]_{V_{ds}\ \text{constant}}$$

and

$$g_d = \left[\frac{dI_{ds}}{dV_{ds}}\right]_{V_{gs}\ \text{constant.}} \tag{40}$$

III. Results and Discussions

Numerical calculations have been performed to evaluate the two photovoltages, the total channel charge, the drain-source current, the channel conductance and the transconductance of the GaAs OPFET with opaque gate under ac condition. The device parameters and values of different constants have been listed in Table I.

Fig. 2(a) and (b) shows the plots of external and internal photovoltages against signal frequency at different optical flux densities. Both external photovoltage (v_{op1}) and internal photovoltage (v_{op2}), remain more or less constant and independent of signal frequency upto 1 MHz. Above 1 MHz the values of v_{op1} and v_{op2} decrease with the increase in the modulating frequency. These variations of photovoltages are similar to those reported by earlier workers [4]. v_{op2} is larger than v_{op1} for a particular flux density and frequency. This is because the reverse saturation current density in the active layer-substrate junction is less compared to that for the Schottky junction. Further, the number of holes generated in the side walls of the Schottky depletion region is much less than that generated in the n–p junction depletion region. The reason for the constant photovoltage upto 1 MHz is that the ac lifetime for holes (16) is constant when $1/\tau_p \gg \omega$. It starts decreasing for $\omega \geq 1/\tau_p$.

Fig. 3 represents the variation of total channel charge with frequency for different flux densities. At a particular frequency, channel charge increases with the increase in flux density. For a particular incident, optical flux density the channel charge remains unchanged upto 0.1 MHz after which it decreases with the increase in frequency. Here the ac lifetime for electrons play the important role. The charge is constant for $1/\tau_n \gg \omega$ and when $\omega \geq 1/\tau_n$ it starts reducing with frequency.

The current versus voltage (I–V) characteristics of the device for different signal frequencies is shown in Fig. 4. With the increase in frequency the drain-source current decreases which is similar to the observation already reported [4].

Fig. 5 represents the I–V characteristics of the present model and that of Zebda *et al.* [8] at a frequency of 0.1 GHz and flux density 10^{21}/m^2-s. The present model shows much higher current because in [8] the effect of photovoltage has not been taken into account which contributes more prominently to the enhancement of the drain-source current, because of channel width modulation. The plot of I_{ds} versus frequency is shown in Fig. 6. It is observed that with the increase in frequency the drain-source current gradually decreases, the change being 0.44 mA/decade at a frequency of 10^9 Hz. The opaque gate model is more frequency sensitive compared to the previous results [4], where the change is 0.03 mA/decade. The better sensitivity of the device to frequency changes in the present model is due to the substrate effect which is not considered in [4].

The variation of transconductance of the device with frequency is plotted in Fig. 7. Transconductance remains constant upto 10^5 Hz and decreases rapidly above that frequency. With the increase in flux density the transconductance increases but beyond 10^{10} Hz it remains more or less unaffected by a change in the flux density.

TABLE I
Values of Different Parameters Assumed for Calculation

Values of different parameters assumed for calculation

Parameter	Name	Value	Unit
σ	Straggle Parameter	0.383×10^{-7}	(m)
R_p	Projected Range	0.861×10^{-7}	(m)
μ_n	Electron Mobility	0.45	(m^2/V.s)
μ_p	Hole Mobility	0.04	(m^2/V.s)
Z	Channel Width	100×10^{-6}	(m)
α	Absorption Coefficient	1.0×10^{6}	(m^{-1})
τ_n	Electron Lifetime	1.0×10^{-6}	(s)
τ_p	Hole Lifetime	1.0×10^{-8}	(s)
v_y	Carrier velocity in y-direction	1.2×10^{5}	(m/s)
t	Thickness of the MESFET including substrate	1.0×10^{-6}	(m)
L	Channel Length	3.0×10^{-6}	(m)
a	active layer thickness	0.15×10^{-6}	(m)
Δ	Position of fermi level below the conduction band	0.02	(ev)
ϕ_B	Schottky barrier height	0.9	(ev)
ε_0	Permittivity	1.04335×10^{-10}	(F/m)
N_t	Trap density	1.0×10^{15}	(m^{-2})
k_p	Capture factors for holes	3.1×10^{-17}	(m^3/s)
k_n	Capture factors for electrons	3.1×10^{-15}	(m^3/s)
v_p	Pinch-off voltage	1.68	V
v_{bs}	Substrate Potential	0.0	V
N_A	Substrate doping conc.	1.0×10^{20}	m^{-3}
N_{dr}	Equivalent const.doping conc.	0.658×10^{23}	m^{-3}

The channel conductance of the device is also calculated and plotted against frequency (Fig. 8) for different flux densities. The channel conductance decreases with the increase in modulating frequency above 0.1 MHz and below 0.1 MHz it remains more or less independent of frequency. Hence it is observed that upto 0.1 MHz the device intrinsic parameters remain unaffected by the signal frequency and above 0.1 MHz when $\omega \geq 1/\tau_n$ the intrinsic parameters start decreasing with frequency.

IV. Conclusion

An ac analysis of the commercial GaAs MESFET with implanted profile having opaque gate has been carried out considering Gaussian distribution of impurity profile under the illuminating condition. The signal modulated light enters the device through the spacings of source, gate and drain. We consider the carrier generation in the side walls of the gate depletion region, the channel neutral region and the n–p junction depletion region (the substrate is assumed to be totally depleted).

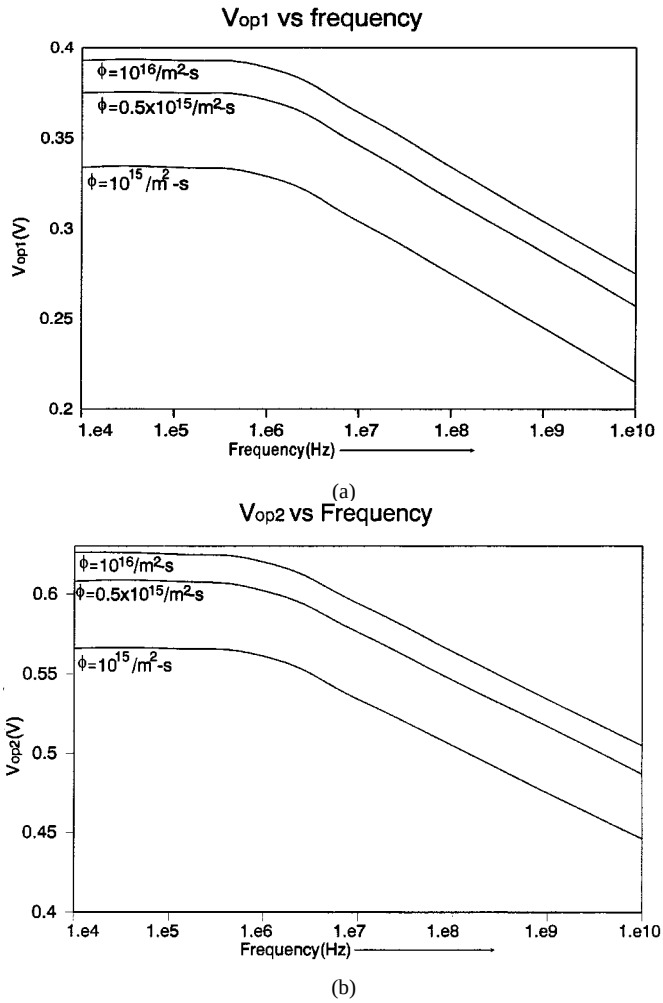

Fig. 2. (a) Variation of external photovoltage with frequency under different flux densities. (b) Variation of internal photovoltage with frequency under different flux densities.

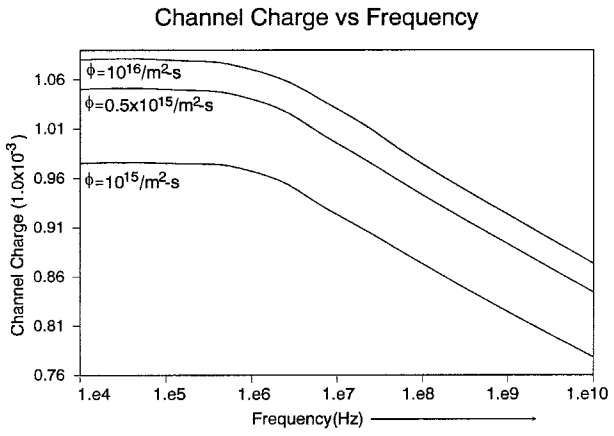

Fig. 3. Channel charge versus frequency for varying flux densities.

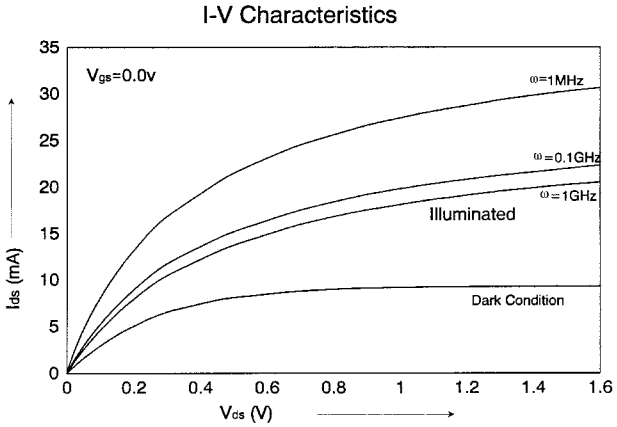

Fig. 4. I–V characteristics of the device for different signal frequencies.

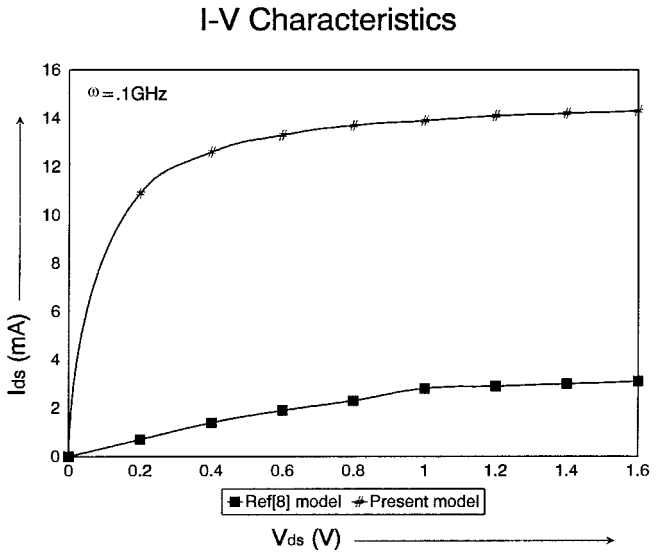

Fig. 5. Comparison of I–V characteristics of the present model with those of [8].

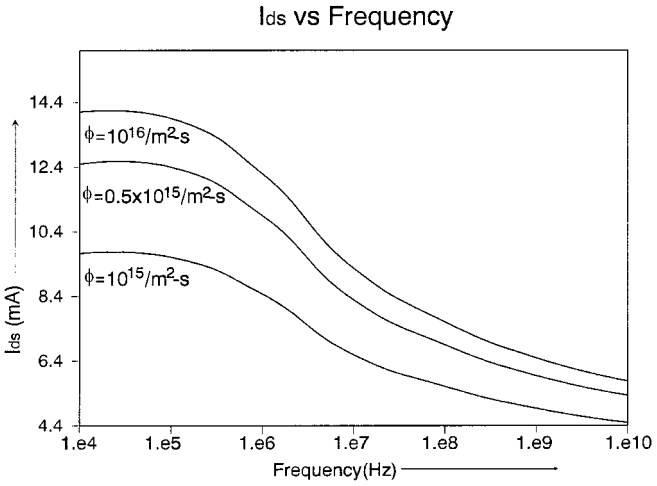

Fig. 6. Drain-source current against frequency for varying flux densities.

Results show significant effect of frequency on the device characteristics. The photovoltages: the external photovoltage across the Schottky junction and the internal photovoltage across the channel- substrate junction reduce with the signal frequency. The I–V curves, g_d–ω and g_m–ω curves show that I_{ds}, g_d, and g_m are independent of frequency upto 1 MHz above which they reduce sharply with frequency. This nature of variation is similar as reported in [4] and is due to the ac lifetime of the carriers. I–V characteristics has also been compared with those of [8] and the discrepancies have been explained. Even though the

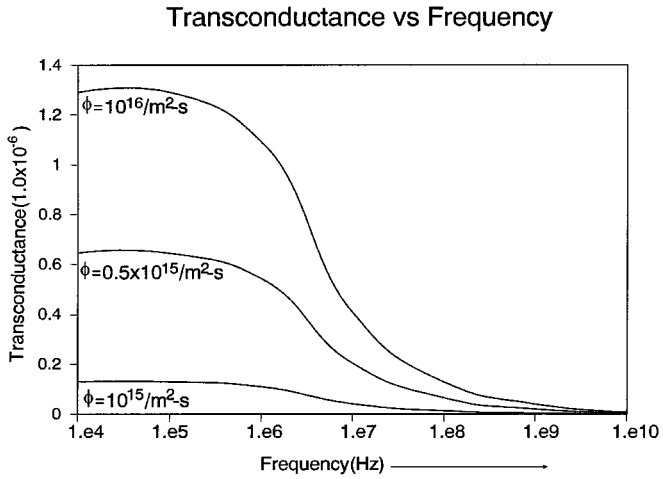

Fig. 7. Transconductance versus frequency for different incident flux densities.

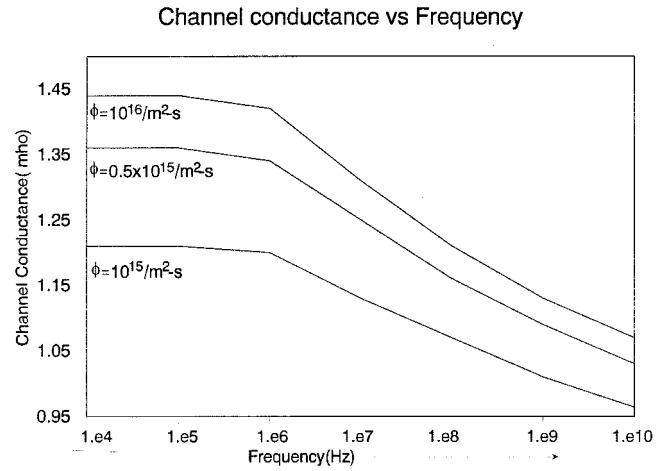

Fig. 8. Channel conductance versus frequency for different flux densities.

results are similar to other published theoretical work, the ac analysis is new for the opaque gate model of GaAs MESFET under illumination. Experimental results on the frequency dependence of GaAs MESFET characteristics under illumination are also available. However, they are mostly on the measurements of S- and Y-parameters of the device [11], [12] which is beyond the scope of the present paper.

APPENDIX

The drain-source current due to ion-implanted profile is given by (33) in which the terms I_1 and I_2 are defined as

$$I_1 = \int_0^{v_D} \operatorname{erf}\left(\frac{y'_{dg} - R_p}{\sigma\sqrt{2}}\right) dv$$
$$I_2 = \int_0^{v_D} \operatorname{erf}\left(\frac{y'_{ds} - R_p}{\sigma\sqrt{2}}\right) dv.$$

They are evaluated as

$$I_1 = \frac{2\sigma^2 q N_D}{\varepsilon}\left[\frac{a_2}{2}\left\{-a_2 \operatorname{erf} a_2 - \frac{1}{\sqrt{\pi}}\left(e^{-a_2^2} - 1\right)\right\}\right.$$
$$+ \frac{a'_2}{2}\left\{a'_2 \operatorname{erf} a_2 + \frac{1}{\sqrt{\pi}}\left(e^{-a_2'^2} - 1\right)\right\}$$
$$\left.+ \frac{1}{4}\{\operatorname{erf} a_2 - \operatorname{erf} a'_2\} + \frac{1}{2\sqrt{\pi}}(a'_2 - a_2)\right]$$
$$I_2 = \frac{q\sigma\sqrt{2}N_{dr}^2}{\varepsilon N_A}\left[(R_p - a)\left\{-a_3 \operatorname{erf} a_3 - \frac{1}{\sqrt{\pi}}\left(e^{-a_3^2} - 1\right)\right.\right.$$
$$+ a'_3 \operatorname{erf} a'_3 + \frac{1}{\sqrt{\pi}}\left(e^{-a_3'^2} - 1\right)\Big\}$$
$$+ \sigma\sqrt{2}\left\{\frac{a'_3}{2}\left(a'_3 \operatorname{erf} a'_3 + \frac{e^{-a_3'^2}}{\sqrt{\pi}}\right)\right.$$
$$- \frac{a_3}{2}\left(a_3 \operatorname{erf} a_3 + \frac{e^{-a_3^2}}{\sqrt{\pi}}\right) - \frac{1}{4}(\operatorname{erf} a'_3 - \operatorname{erf} a_3)$$
$$\left.\left.+ \frac{1}{\sqrt{\pi}}(a'_3 - a_3)\right\}\right].$$

In the above expressions

$$a_2 = \frac{[y'_{dg}]_{v=0} - R_p}{\sigma\sqrt{2}}$$
$$a_3 = \frac{[y'_{ds}]_{v=0} - R_p}{\sigma\sqrt{2}}$$
$$a'_2 = \frac{[y'_{dg}]_{v=v_{ds}} - R_p}{\sigma\sqrt{2}}$$
$$a'_3 = \frac{[y'_{ds}]_{v=v_{ds}} - R_p}{\sigma\sqrt{2}}.$$

In (34), the drain-source current due to generation of carriers in the neutral channel region has the terms I_3, I_4, I_5, and I_6. They are expressed as

$$I_3 = \frac{qN_{dr}L_{n\omega}^2}{\varepsilon}\{\exp B(B-1) - \exp B1(B1-1)\}$$
$$I_4 = \frac{qN_{dr}^2 L_{n\omega}}{\varepsilon N_A}\{\exp(C1)[(C1-1)L_{n\omega} + a]$$
$$- \exp(C2)[(C2-1)L_{n\omega} + a]\}$$
$$I_5 = \frac{qN_{dr}^2}{\varepsilon\alpha N_A}\left\{\exp(D)\left[a + \frac{D}{\alpha} - \frac{1}{\alpha}\right]\right.$$
$$\left. - \exp(D1)\left[a + \frac{D1}{\alpha} - \frac{1}{\alpha}\right]\right\}$$
$$I_6 = \frac{qN_{dr}}{\varepsilon\alpha^2}\{\exp(E)(E-1) - \exp(E1)(E1-1)\}$$

where

$$B = -\frac{[y_{dg}]_{V=V_{ds}}}{L_{n\omega}} \qquad B1 = -\frac{[y_{dg}]_{V=0}}{L_{n\omega}}$$
$$C1 = -\frac{[y_{ds}]_{V=V_{ds}}}{L_{n\omega}} \qquad C2 = -\frac{[y_{ds}]_{V=0}}{L_{n\omega}}$$
$$D = -\alpha[y_{ds}]_{V=V_{Ds}} \qquad D1 = -\alpha[y_{ds}]_{V=0}$$
$$E = -\alpha[y_{dg}]_{V=V_{DS}} \qquad E1 = -\alpha[y_{dg}]_{V=0}.$$

I_7 and I_8 in (37) are of the form

$$I_7 = \frac{N_{dr}^2}{N_A}\left[e^D\left(\frac{D}{\alpha} - \frac{1}{\alpha} - a\right) - e^{D1}\left(\frac{D1}{\alpha} - \frac{1}{\alpha} - a\right)\right]$$

$$I_8 = \frac{1}{N^2}\left[e^F\left(\frac{F}{\alpha} - \frac{1}{\alpha} - a\right) - e^{F1}\left(\frac{F1}{\alpha} - \frac{1}{\alpha} - a\right)\right].$$

In the above expression F and $F1$ are written as

$$F = -\alpha[y_w]_{V=V_{ds}} \quad \text{and} \quad F1 = -\alpha[y_w]_{V=0}.$$

N is the equivalent concentration of p-n region given by

$$\frac{1}{N} = \frac{1}{N_A} + \frac{1}{N_{dr}}.$$

REFERENCES

[1] C. Baack, G. Elze, and G. Walf, "GaAs MESFET: A high speed optical detector," *Electron. Lett.*, vol. 13, no. 7, p. 193, Mar. 1977.

[2] H. Mizuno, "Microwave characteristics of an optically controlled GaAs MESFET," *IEEE Trans. Microwave Theory Tech.*, vol. MTT-31, pp. 596–600, July 1983.

[3] S. Mishra, V. K. Singh, and B. B. Pal, "The effect of surface recombination on the frequency dependent characteristics of an ion-implanted GaAs OPFET," *IEEE Trans. Electron Devices*, vol. 37, pp. 942–946, Apr. 1990.

[4] B. B. Pal, Shubha, K. Kumar, and R. U. Khan, "Frequency dependent behavior of an ion-implanted GaAs OPFET considering photovoltaic effect and the gate depletion width modulation," *Solid State Electron.*, vol. 38, no. 5, pp. 1097–1102, 1995.

[5] Shubha, B. B. Pal, and R. U. Khan, "Optically controlled ion-implanted GaAs MESFET characteristic with opaque gate," *IEEE Trans. Electron Devices*, vol. 45, pp. 78–84, Jan. 1998.

[6] G. W. Taylor, H. M. Darley, and P. K. Chatterjee, "A device model for an ion-implanted MESFET," *IEEE Trans. Electron Devices*, vol. ED-26, pp. 172–182, Mar. 1979.

[7] B. B. Pal and S. N. Chattopadhyay, "GaAs OPFET characteristics considering the effect of gate depletion modulation due to incident radiation," *IEEE Trans. Electron Devices*, vol. 39, pp. 1021–1027, May 1992.

[8] Y. Zebda and S. Abu Helweh, "AC characteristics of optically controlled MESFET (OPFET)," *J.Lightwave Technol.*, vol. 15, pp. 1205–1211, July 1997.

[9] S. M. Sze, *Physics of Semiconductor Devices*, 2nd ed. New Delhi, India: Wiley Eastern Ltd., 1983, pp. 755–755.

[10] Shubha, R. B. Lohani, B. B. Pal, and R. U. Khan, "A generalized D.C model for GaAs OPFET considering ion implanted profile," *Optic. Eng.*, vol. OPD.ENG. 37, no. 4, pp. 1343–1352, Apr. 1998.

[11] R. N. Simons, "Microwave performance of an optically controlled AlGaAs/GaAs high electron mobility transistor and GaAs MESFET," *IEEE Trans. Microwave Theory Tech.*, vol. MTT-35, pp. 1444–1455, Dec. 1989.

[12] S. Kawasaki, H. Shiomi, and K. Matsugatani, "A novel FET model including an illumination-intensity parameter for simulation of optically controlled millimeter-wave oscillators," *IEEE Trans. Microwave Theory Tech.*, vol. 46, pp. 820–828, June 1998.

Nandita Saha Roy received the B.Sc. and M.Sc. degrees in physics from Banaras Hindu University, Varanasi, India, in 1993 and 1995, respectively. Presently, she is working toward the Ph.D. degree on high speed devices.

In September 1995, she joined the Department of Electronics Engineering, Institute of Technology, Banaras Hindu University as a Research Scholar.

B. B. Pal is a Professor at the Centre of Advanced Study, Department of Electronics Engineering, Institute of Technology, Banaras Hindu University, Varanasi, India.

R. U. Khan received the B.E., M.E., and Ph.D. degrees in electronics engineering from the Institute of Technology, Banaras Hindu University, Varanasi, India, in 1971, 1973, and 1987, respectively.

He joined the Department of Electronics Engineering, Institute of Technology, Banaras Hindu University, (India) as a Lecturer in 1980. The present areas of interest are millimeter-wave solid-state devices, MESFET's, MOSFET's, and III–V semiconductor compounds. He has published more than 30 papers in journals and conference proceedings.

Dr. Khan received the Foundation life membership of the Semiconductor Society of India.